


Handbook  
for  
Generic Photonic IC Design

Editors: Meint Smit and Xaveer Leijtens

4-4-2026

 *Handbook for generic photonic IC design*, by the *Photonic Integration group*, Technische Universiteit Eindhoven, is licensed under a Creative Commons “Attribution-NonCommercial-NoDerivatives 4.0 International” license.

We traced the ownership of all figures used as far as we could. However, if you are a copyright owner and believe we used your work without permission, please contact us at [coordinator@jeppix.eu](mailto:coordinator@jeppix.eu).

## Chapter 23

# Star Couplers

MEINT SMIT

### 23.1 Introduction

A star coupler can be considered as an extension of a Y-junction, in which the input light is coupled to a larger number of waveguides. It is an essential part in Optical Phased Arrays and Arrayed Waveguide Gratings, where it is responsible for a number of performance parameters, such as the insertion loss, the coupling uniformity and the side lobe level. *star coupler*

### 23.2 Coupler geometry and beam shape

Figure 23.1 illustrates the coupler geometry. If the coupler is well designed the insertion loss can be very low. At the end of the transmitter-waveguide the waveguide mode transforms in an almost lossless way into a divergent beam due to diffraction. Because for customary waveguides with V-parameters in the range from 2-5 the waveguide mode  $U_0(y)$  closely resembles a Gaussian beam, the divergent beam in the Free Propagation Region (FPR) can be described in good approximation as a Gaussian beam (see Chapter 2 Sec2.4.8). So the field  $U_f(\theta)$  at the aperture of the array will also have a Gaussian distribution. If the gaps between the array waveguides are infinitely sharp the input field will couple smoothly into the waveguide array and transform adiabatically into a set of uncoupled waveguide modes, the amplitudes of which are proportional to the amplitude of the field at the input of the waveguides. They will thus also have a Gaussian distribution. Because the adiabatic evolution from the Gaussian input field  $U_f$  to the set of uncoupled waveguide modes is lossless the insertion loss of the star coupler can be very low. Much lower than 1 dB, in principle, if the array is wide enough to intercept the largest part of the beam. For the lowest insertion loss the FPR should have the same vertical waveguide structure as the waveguides. In Fig. 23.1 the waveguides are depicted for reasons of clarity as if they stop at FPR. In reality they connect seamlessly to the FPR as depicted in Fig. 23.2. *Gaussian beam*  
*Free Propagation Region*  
*adiabatic*

The Gaussian distribution of the mode amplitudes in the array can be an advantage or a disadvantage, dependent on the application. If the star coupler is used as power divider for an optical phased array for beam steering or an Arrayed Waveguide Grating,

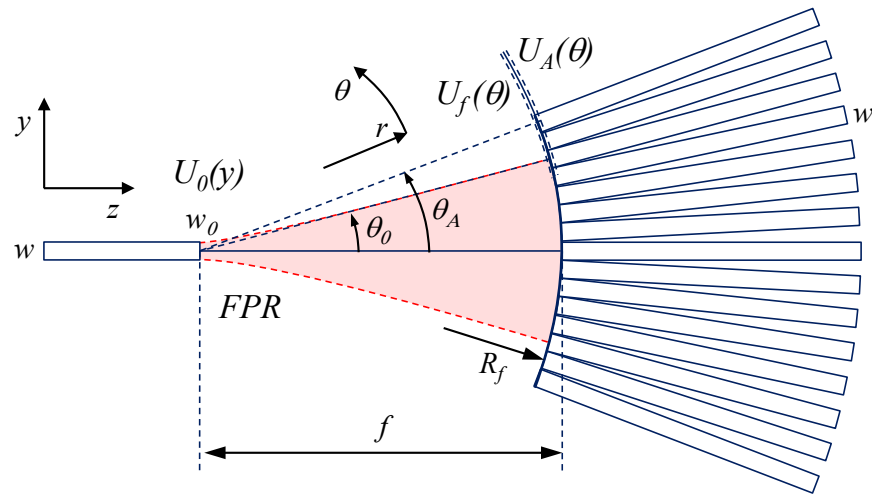


Figure 23.1: Star coupler geometry

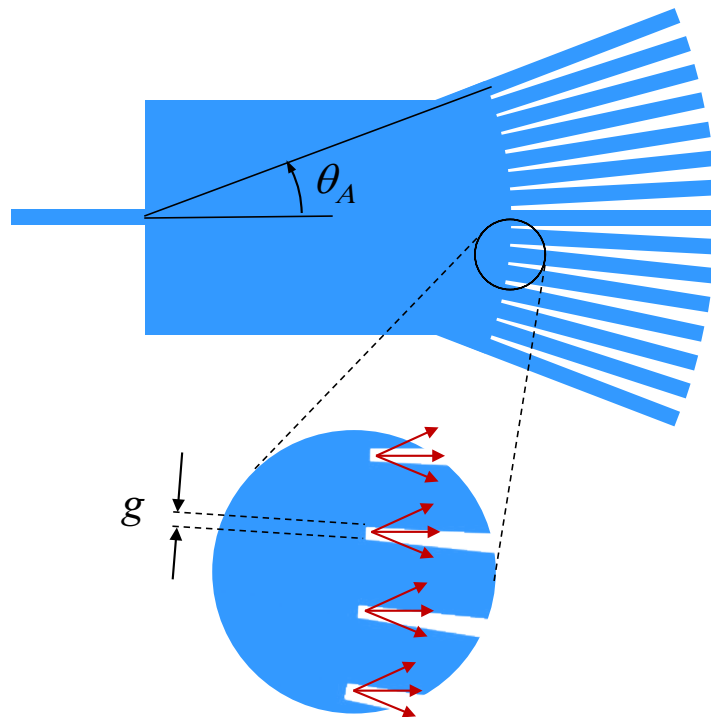
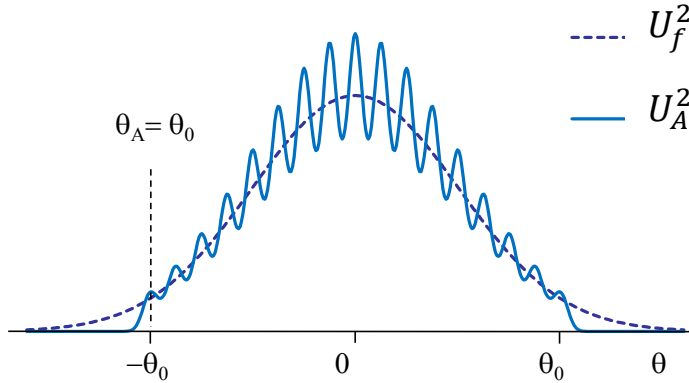


Figure 23.2: Discontinuity between the array and the Free Propagation Region due to the finite resolution of the lithography, which causes an abrupt closure of the gap at gap width  $g$ .



**Figure 23.3:** The exciting field intensity  $U_f^2$  just before and the guided field intensity  $U_A^2$  just after the junction between the FPR and the array.

the Gaussian distribution is advantageous because it will produce a focal field or a far field with a low side-lobe level. If we want a uniform power splitting, the star coupler is less ideal. We can control the power division to some extent by increasing the width of the array waveguide towards the edges of the array, using a taper. The possible correction is limited, however, and we will have to accept that part of the power in the edge of the beam will not be captured by the array.

The main source of loss for a star coupler is caused by the finite resolution of the lithography and the etching process. This finite resolution will cause the gap between the waveguides to close abruptly as soon as it becomes smaller than the resolution, similar to the gap closure in a Y-junction. This gap closure causes a discontinuity at which part of the beam power will be scattered or reflected, as depicted in Fig. 23.2.

*gap closure*

In the following paragraphs we will analyse the most important properties of the coupler using a Gaussian approximation of the mode and the divergent beam. We approximate the modal field of the transmitter waveguide as:

$$U_0(y) = A e^{-y^2/w_0^2} \quad (23.1)$$

in which  $w_0 = w_e \sqrt{2/\pi}$  and  $w_e \approx w \{0.5 + 1/(V - 0.6)\}$  as explained in 2.4.7.  $V$  is the lateral V-parameter of the transmitter waveguide. In the Free Propagation Region (FPR) the mode expands through diffraction into a divergent beam, which is also Gaussian:

$$U(\theta) = B e^{-\theta^2/\theta_0^2} \quad (23.2)$$

in which  $\theta_0 = \lambda_0 / (N_{FPR} \pi w_0)$ . At a distance  $f$  from the transmitter waveguide the beam has a width  $w_f = f \cdot \theta$  and a radius  $R_f = f \sqrt{1 + (z_0/f)^2}$  in which the focal half depth  $z_0 = w_0/\theta_0$ . The radius  $R_f$  of the equiphase front at a distance  $f$  of the transmitter waveguide is slightly larger than  $f$ . To excite all waveguides with the same phase the radius of the input aperture should be  $R_f$  rather than  $f$ .

### 23.3 Array coupling loss

As mentioned above the main source of loss for a star coupler is caused by the discontinuity between the FPR and the point where the array starts. With an infinitely good

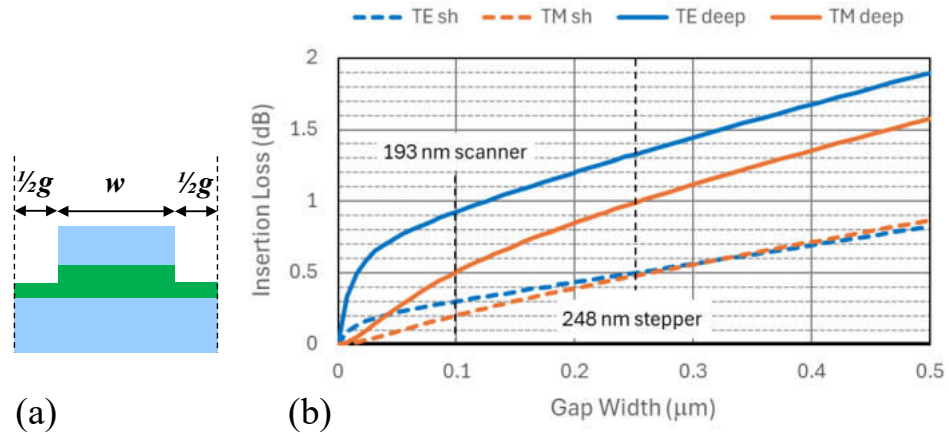


**Figure 23.4:** The insertion loss of TE- and TM-polarized modes at the junction between the Free Propagation Region and a deep and shallow etched waveguide array, as a function of the gap-width. The dashed vertical lines indicate the minimum gap that can be obtained with a 193 nm scanner and a 248 nm stepper.

resolution there would be no discontinuity and hence no loss. But because of the finite resolution the FPR will transform abruptly into an array with a finite gap width. Before the interface the field will have the Gaussian profile  $U_f(\theta)$ , as shown in Figure 23.3. Directly after the interface the field will be carried by a set of (coupled) waveguide modes which together have a profile  $U_A(\theta)$ , as shown in Fig. 23.3. If the gap increases the field will concentrate in the waveguides and the field between the waveguides will reduce to zero where the gap is sufficiently wide for the waveguides to be decoupled. The latter process is adiabatic and thus loss free. So the main source of loss is the coupling loss which occurs at the interface. It can be found by calculating the overlap integral of the fields at both sides of the interface, as described in 2.7, Eq. 2.115:

$$\eta = \frac{\int |U_f(\theta) \cdot U_A(\theta)|^2 d\theta}{\int |U_f(\theta)|^2 d\theta \cdot \int |U_A(\theta)|^2 d\theta}$$

With proper array design the functions  $U_f(\theta)$  and  $U_A(\theta)$  are real-valued. The calculation of the field  $U_A(\theta)$  requires a numerical field solver. We can get a good approximation of the overlap by restricting the calculation of the overlap to a section with a half waveguide and a half gap, as shown in Fig. 23.4, and assuming symmetry around both boundaries (zero first derivatives of the field).

Fig. 23.4 shows the dependence of the coupling loss on the gap width for the standard shallow and deep etched InP waveguides with waveguide widths 2 and 1.5  $\mu\text{m}$ , respectively. We see that with 193 nm scanner lithography the coupling loss for shallow etched waveguides can become lower than 0.3 dB if we can open the gap down to 100 nm width. This requires very careful proximity correction. With a 250 nm gap, which can be realised with 248 nm stepper lithography, the coupling loss for shallow etched waveguides is still below 0.4 dB.

For deep etched waveguides the coupling loss at the junction is significantly higher, as expected: with 193 nm scanner lithograph close to 1 dB and 0.5 dB for TE- and TM-polarization, respectively. And with 248 nm stepper lithography 1.3 and 1 dB for TE- and TM-polarization, respectively.

Fig. 23.5 shows the dependence of the reflection on the gap width for the standard

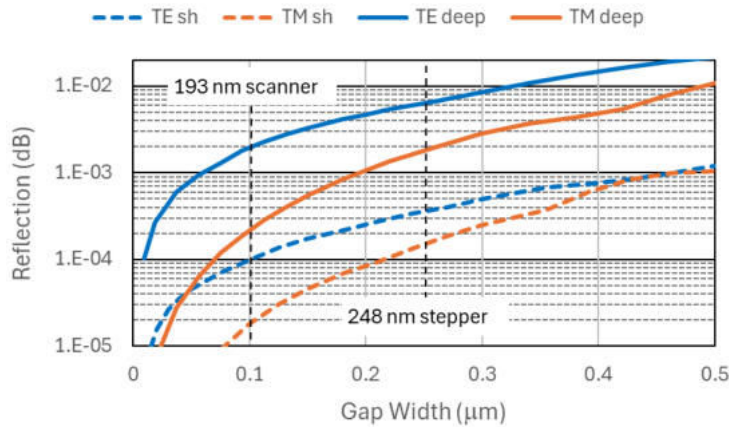


**Figure 23.5:** The reflection of TE- and TM-polarized modes at the junction between the Free Propagation Region and a deep and shallow etched waveguide array .

shallow and deep etched InP waveguides. For the shallow-etched waveguide array the reflection levels for 100 nm gaps (193 nm scanner lithography) are below -40 dB for TE and below -47 dB for TM-polarized light. For 250 nm gaps (248 nm stepper lithography) the reflection levels are -35 and -38 dB for TE and TM, respectively. For the deep etched waveguides the reflection levels are higher, as expected: -22 and -27 for TE and TM, respectively, for a 100 nm gap, and -35 and -38 dB for a 250 nm gap.

In practice the reflection levels may be lower than calculated because due to the lag effect the gap closure will be more gradual than assumed in the calculation. The effect of the gap closure will be that the FPR will become longer by a factor  $g/w$ , but apart from the coupling loss occurring at the discontinuity it will have little effect on the coupler performance. The power lost at the discontinuity will be radiated out of the waveguides. For shallow etched waveguides part of it may propagate through the cladding region beside the waveguides and pop up at other parts of the PIC, where it may couple into waveguides at discontinuities. Usually these crosstalk levels will be very low.

*lag effect  
gap closure*

### 23.4 Truncation loss.

Another loss contribution follows from the finite width of the array aperture. The field  $U_A(\theta)$  in Fig. 23.6 is shown for an array half width  $\theta_A = \theta_0$ . For  $|\theta| > \theta_A$  there are no waveguides and the field  $U_A(\theta)$  drops to zero. The power in the field  $U_f(\theta)$  for  $|\theta| > \theta_A$  is lost. The truncation loss can be estimated from Gaussian beam analysis:

*truncation loss*

$$\begin{aligned} \eta(\theta_A) &= \int_{-\theta_A}^{\theta_A} \hat{U}_f^2(\theta) d\theta \approx \text{erf}\left(\frac{\theta_A}{\theta_0} \sqrt{2}\right) \\ L_A &= 10 \log \eta(\theta_A) \end{aligned} \tag{23.3}$$

in which  $\hat{U}_f^2(\theta)$  is the normalized Gaussian intensity and  $\text{erf}(x)$  is the well known error function  $\text{erf}(x) = (2/\sqrt{\pi}) \int_0^x e^{-x^2} dx$ . The derivation of the formula is given in Problem 23.1. Figure 23.6 shows the truncation loss in dB as a function of  $\theta_A/\theta_0$ . It is seen that for  $\theta_A = \theta_0$  the contribution to the insertion loss is 0.2 dB. So from an insertion loss point of view there is no need to make  $\theta_A > \theta_0$ .

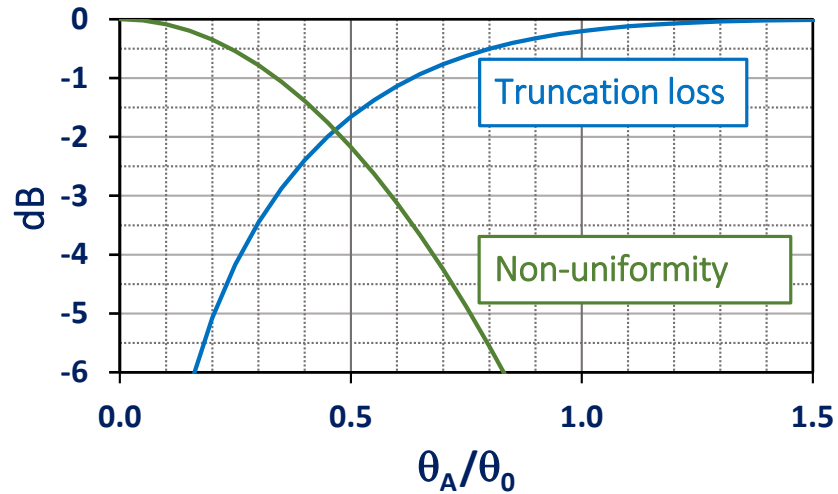


**Figure 23.6:** The dependence of truncation loss and non-uniformity on the array aperture  $\theta_A$ .

**Problem:** Derive formula 23.3.

**Solution:** The coupling efficiency is the fraction of the beam power which is captured in the array. It follows as  $\eta \approx C \int_{-\theta_A}^{\theta_A} U_f^2(\theta) d\theta = 2C \int_0^{\theta_A} e^{-2\theta^2/\theta_0^2} d\theta$  in which C is a normalisation constant. With the substitution  $\theta = u\theta_0/\sqrt{2}$  the integral transforms into:  $\eta \approx C' \int_0^{u_A} e^{-u^2} du = \text{erf}(u_A)$  with  $C' = 1/(\int_0^\infty e^{-u^2} du) = 2/\sqrt{\pi}$ . By substituting  $u_A = (\theta_A/\theta_0)\sqrt{2}$  we arrive at formula 23.1.

**Problem 23.1:** Y-junction design and performance.

## 23.5 Non-uniformity.

The non-uniformity of the power in the array waveguides follows the Gaussian intensity profile at the array aperture, as shown in Fig. 23.3. If we accept a non-uniformity of 3 dB between the star-coupler channels, we see from Fig. 23.6 that we have to choose  $\theta_A = 0.6\theta_0$ . This choice will bring us a truncation loss slightly higher than 1 dB. *non-uniformity*

We can reduce the non-uniformity of the array by making the array waveguides wider towards the edges of the array, in such a way that the product of the intensity and the waveguide width is constant across the aperture, and taper the width adiabatically down to the standard width. In this case all waveguides will receive the same amount of power, but we have to take care for higher-order mode excitation.

## 23.6 Higher order mode excitation.

So far there has been little reported on the excitation of higher-order modes in the array waveguides. They can be excited at the interface between the FPR and the array, and at discontinuities in the array waveguides, for example at the connection between a straight and a curved waveguide. In Optical Phased Arrays (OPAs) and Arrayed Waveguide Gratings (AWGs) they will affect the phase and amplitude transfer of the array. *higher-order mode excitation*

A second-order mode will be excited by a uniform illumination of the waveguide, but will be radiated if it is beyond cut-off in the waveguide. It will contribute to the coupling loss at junction between the FPR and the array, but otherwise it will have little effect on the transmission properties of the array.

A small fraction of the input power will be coupled to the first order mode if the illumination is not symmetric, which is increasingly the case if we get farther away from the center of the array aperture. For a given asymmetry  $dI(\theta)/d\theta$ , in which  $I(\theta) = U^2(\theta)$ , it will increase quadratically with the width of the waveguide. So if we apply tapering towards the edges of the array it may become significant.